Journal of Coordination Chemistry

ISSN: 0095-8972 (Print) 1029-0389 (Online) Journal homepage: http://www.tandfonline.com/loi/gcoo20

Synthesis, structure, and properties of a pentanuclear cobalt(III) coordination cluster

Swamy Maloth, Sathish Kumar Kurapati & Samudranil Pal

To cite this article: Swamy Maloth, Sathish Kumar Kurapati & Samudranil Pal (2015) Synthesis, structure, and properties of a pentanuclear cobalt(III) coordination cluster, Journal of Coordination Chemistry, 68:8, 1402-1411, DOI: 10.1080/00958972.2015.1018195

To link to this article: http://dx.doi.org/10.1080/00958972.2015.1018195

Journal of Coordination Chemistry, 2015
Vol. 68, No. 8, 1402–1411, http://dx.doi.org/10.1080/00958972.2015.1018195

Taylor & Francis
Taylor & Francis Group

Synthesis, structure, and properties of a pentanuclear cobalt(III) coordination cluster

SWAMY MALOTH, SATHISH KUMAR KURAPATI and SAMUDRANIL PAL*

School of Chemistry, University of Hyderabad, Hyderabad, India

(*Received 12 July 2014; accepted 5 January 2015*)

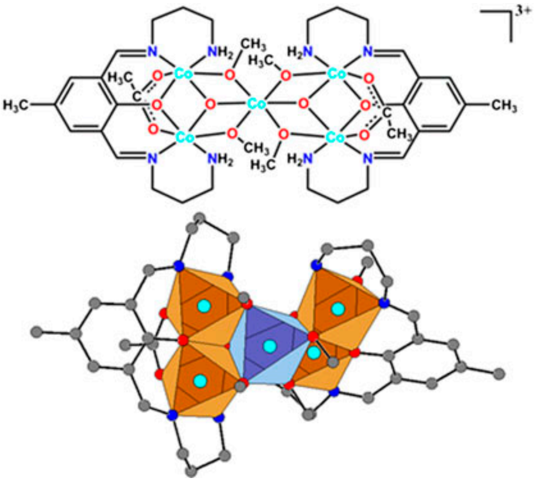

The synthesis, X-ray structure and properties of a pentanuclear cobalt(III) coordination cluster [{L(O$_2$CCH$_3$)Co$_2$O(OCH$_3$)$_2$}$_2$Co](ClO$_4$)$_3$ (**1**) (L$^-$ = 2,6-bis((3-aminopropylimino)methyl)-4-methylphenolate) are described. The dinucleating L$^-$ is coordinated with two cobalt(III) centers to form the {L(O$_2$CCH$_3$)Co$_2$O(OCH$_3$)$_2$} unit, where each metal center is in a distorted octahedral N$_2$O$_4$ environment. The oxo and the methoxo ligands of these two dinuclear units assemble a distorted octahedral O$_6$ coordination sphere around the central cobalt(III). Elemental analysis and spectroscopic (IR, NMR, UV–vis, and HRMS) features are consistent with the pentanuclear structure of the complex. The diamagnetic complex is a 1 : 3 electrolyte in solution. It is redox-active and displays a metal-centered reduction at $E_{1/2} = -0.04$ V (*vs*. Ag/AgCl).

Keywords: Pentanuclear complex; Cobalt(III); Dinucleating ligand; Crystal structure; Physical properties

---

*Corresponding author. Email: spal@uohyd.ac.in

1. Introduction

Polynuclear transition metal coordination clusters are of interest due to their potential applications in catalysis, photonics, electrochemistry, molecular magnetism, and their biological activity [1–12]. Their diverse applications arise from the physical properties that can be attributed to their molecular architectures. Consequently, there is interest in synthesizing new structurally intricate transition metal coordination clusters. The nuclearity and topology of such a cluster, and hence its overall molecular architecture is generally determined by the type of ligands used. Acyclic compartmental Schiff bases derived from 2,6-diformyl-4-methylphenol or analogous dialdehydes provide complexes with a bimetallic core that is supported by various additional ancillary bridging ligands such as oxide, hydroxide, alkoxide, halide, and carboxylate. Self-assembly of this type of dinuclear complex via formation of additional bridges by the ancillary ligands of the primary dinuclear unit or by small bridging ligands can lead to extended polynuclear coordination clusters involving additional metal cations [13–17]. The magnetic properties of cobalt(II) have led to considerable interest in cobalt(II) coordination clusters as single molecule magnets [10, 11, 17–25]. In an attempt to prepare a coordination cluster using cobalt(II) acetate and the acyclic compartmental Schiff base 2,6-bis((3-aminopropylimino)methyl)-4-methylphenol, we have isolated the diamagnetic pentanuclear cobalt(III) species $[\{L(O_2CCH_3)Co_2O(OCH_3)_2\}_2Co]^{3+}$. Herein, we describe the synthesis, characterization, crystal structure, and spectroscopic properties of the perchlorate salt of this complex cation.

2. Experimental

2.1. *Materials*

All chemicals and solvents used in this work were of reagent grade and were used as received.

2.2. *Physical measurements*

A Thermo Finnigan Flash EA1112 series elemental analyzer was used for the elemental (C, H, and N) analysis measurements. A Sherwood Scientific balance was used for magnetic susceptibility measurement. Solution electrical conductivity was measured using a Digisun DI-909 conductivity meter. The mass spectrum was obtained using a Bruker Maxis HRMS (ESI-TOF analyzer) spectrometer and the infrared spectrum was recorded using a Thermo Scientific Nicolet 380 FT-IR spectrometer. A Shimadzu UV-3600 UV–Vis–NIR spectrophotometer was used to collect the electronic spectrum. The ^1H (400 MHz) NMR spectrum was recorded using a Bruker NMR spectrometer. A CH Instruments model 620A electrochemical analyzer was used for the cyclic voltammetric measurements.

2.3. *Synthesis of $[\{L(O_2CCH_3)Co_2O(OCH_3)_2\}_2Co](ClO_4)_3$ (1)*

A solution of 2,6-diformyl-4-methyl-phenol (50 mg, 0.3 mM) in CH_3OH (10 mL) was added dropwise over a period of 10 min to a solution of 1,3-diaminopropane (0.05 mL, 44 mg, 0.6 mM) in CH_3OH (10 mL), and the mixture was stirred at room temperature for 1 h. To the resulting yellow solution, solid $Co(O_2CCH_3)_2{\cdot}4H_2O$ (187 mg, 0.75 mM) was added in one portion and the solution was stirred for 10 min. The yellow color of the reaction mixture turned dark brown. To this brown solution, a CH_3OH solution (5 mL) of $NaClO_4{\cdot}H_2O$ (85 mg, 0.6 mM) was added and the mixture was refluxed for 6 h. The solution was then cooled to room temperature and allowed to evaporate slowly to approximately half of the initial volume in 2 days. The resultant dark brown needle-shaped crystals were collected by filtration. This material was recrystallized three times from a $CH_3CN–C_6H_5CH_3$ mixture (20 mL, 1 : 3 ratio) to remove the cobalt(II) impurity. The recrystallized product was dried in air, crushed to give a powder, and stored under vacuum. The yield of the dark green powder varied from 50 to 64 mg (24–30%) and was used for elemental analysis, spectroscopic, and electrochemical measurements. Anal. Calcd for $Co_5C_{38}H_{64}N_8O_{24}Cl_3$: C, 32.19%; H, 4.55%; N, 7.90%. Found: C, 32.25%; H, 4.48%; N, 7.81%. UV–vis data in CH_3CN (λ_{max} (nm) (ε (10^4 M^{-1} cm^{-1}))): 365 (1.9), 305sh (3.4), 250sh (9.1), 213 (13.2).

2.4. *X-ray crystallography*

Complex **1** crystallizes as **1**$\cdot C_6H_5CH_3$ as well as **1**$\cdot C_6H_5CH_3{\cdot}CH_3CN$ from the $CH_3CN–C_6H_5CH_3$ (1 : 3) solution. X-ray data for **1**$\cdot C_6H_5CH_3$ and **1**$\cdot C_6H_5CH_3{\cdot}CH_3CN$ were collected on a Bruker-Nonius SMART APEX CCD and Oxford Diffraction Xcalibur Gemini single crystal X-ray diffractometers, respectively, using graphite monochromated-Mo *Kα* radiation (λ = 0.71073 Å). Data were collected at 100 K for both crystals. The SMART and the SAINT-Plus packages [26] were used for data acquisition and data extraction, respectively, and SADABS [27] was used for the absorption correction for **1**$\cdot C_6H_5CH_3$. The CrysAlisPro software [28] was used for data collection, reduction, and absorption correction

Table 1. Crystallographic data for **1**$\cdot C_6H_5CH_3$ and **1**$\cdot C_6H_5CH_3{\cdot}CH_3CN$.

Complex	**1**$\cdot C_6H_5CH_3$	**1**$\cdot C_6H_5CH_3{\cdot}CH_3CN$
Empirical formula	$C_{45}H_{72}N_8O_{24}Cl_3Co_5$	$C_{47}H_{75}N_9O_{24}Cl_3Co_5$
Formula weight	1510.13	1551.16
Crystal system	Monoclinic	Monoclinic
Space group	$P2_1/n$	$P2_1/n$
T (K)	100	100
a (Å)	17.095(2)	12.7197(9)
b (Å)	16.640(2)	27.992(3)
c (Å)	21.531(3)	17.2725(19)
β (°)	99.744(2)	92.277(5)
V (Å^3)	6036.6(15)	6145.0(10)
Z	4	4
D_{Calcd} (g cm^{-3})	1.662	1.677
μ (mm^{-1})	1.563	1.538
Collected reflns.	57,220	29,063
Unique reflns.	10,645	10,797
Obsd. reflns. [$I \geq 2\sigma(I)$]	9123	7659
Goodness-of-fit on F^2	1.067	1.039
R_1, wR_2 [$I \geq 2\sigma(I)$]	0.0440, 0.1294	0.0574, 0.1329
R_1, wR_2 (all data)	0.0511, 0.1355	0.0898, 0.1494
$\Delta\rho_{max}$, $\Delta\rho_{min}$ (e Å^{-3})	1.068, −0.668	1.435, −0.913

for **1**·$C_6H_5CH_3$·CH_3CN. The structures were solved by direct methods and refined on F^2 by a full-matrix least-squares procedure. In each structure, all non-hydrogen atoms were refined using anisotropic thermal parameters. The hydrogens were included in the structure factor calculation at idealized positions using a riding model. Structure solution and refinement were performed using the SHELX-97 programs [29] available in the WinGX package [30]. The Platon [31] and Mercury [32] packages were used for molecular graphics. Selected crystallographic data are summarized in table 1.

3. Results and discussion

3.1. *Synthesis and some properties*

The one-pot reaction of 2,6-diformyl-4-methylphenol, 1,3-diaminopropane, cobalt(II) acetate, and sodium perchlorate in a 2 : 4 : 5 : 4 mole ratio in CH_3OH under aerobic conditions gives $[\{L(O_2CCH_3)Co_2O(OCH_3)_2\}_2Co](ClO_4)_3$ (**1**) in 24–30% yield. The elemental analysis data are consistent with the molecular formula of **1**. Solid-state magnetic susceptibility measurement provides support for a diamagnetic complex. The molar conductivity Λ_M (380 Ω^{-1} cm^2 M^{-1}) of **1** in CH_3CN is within the range expected for a 1 : 3 electrolyte [33]. The positive-ion ESI mass spectrum of **1** (figure 1) shows three characteristic peaks with the expected isotopic patterns at $m/z = 373.03$, 609.03, and 1316.99 corresponding to the triple-charged cationic complex, a double-charged complex incorporating a perchlorate anion, and a single-charged complex incorporating two perchlorate anions, respectively. The diamagnetic nature, the 1 : 3 electrolytic behavior and the mass spectral features clearly establish the +3 oxidation state and low-spin state of the five cobalt centers in **1**. The cobalt centers are oxidized from +2 to +3 by aerial oxidation during synthesis of the complex from cobalt(II) acetate.

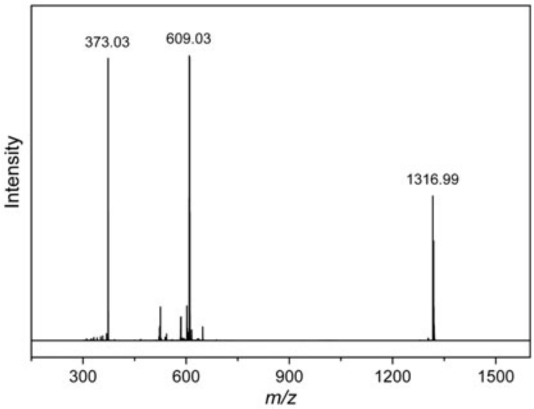

Figure 1. ESI mass spectrum of $[\{L(O_2CCH_3)Co_2O(OCH_3)_2\}_2Co](ClO_4)_3$ (**1**).

3.2. *Crystal structure*

X-ray quality crystals of the complex were grown by slow evaporation from a CH_3CN–$C_6H_5CH_3$ (1 : 3) solution. **1**·$C_6H_5CH_3$ was crystallized on a single occasion, with all other crystallization attempts resulting in the crystallization of **1**·$C_6H_5CH_3$·CH_3CN. X-ray data were collected for both crystals. The thermal ellipsoid plot of the $[\{L(O_2CCH_3)Co_2O(OCH_3)_2\}_2Co]^{3+}$ core of **1** is illustrated in figure 2. The differences in the bond parameters of the tricationic complex in the two structures are statistically insignificant. In general, all metal-to-ligand bond lengths in **1** (table 2) are within the ranges reported for cobalt(III) complexes with similar coordinating atoms [17–20, 34–39]. The bond parameters in the dinuclear $\{L(O_2CCH_3)Co_2O(OCH_3)_2\}$ units with the metal centers having distorted octahedral N_2O_4 geometries are comparable. L^- coordinates to two cobalt(III) centers via a bridging phenolate-O, two imine-N, and two amine-N donors forming fused 6,6,6,6-membered chelate rings. An acetate and an oxo group provide two additional bridges between the two metal centers. The remaining coordination site of each cobalt(III) is occupied by a methoxo

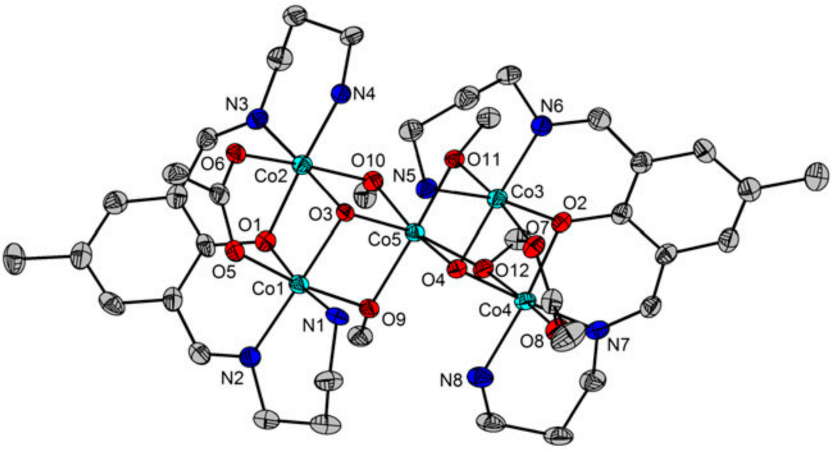

Figure 2. Thermal ellipsoid plot for $[\{L(O_2CCH_3)Co_2O(OCH_3)_2\}_2Co]^{3+}$ (thermal ellipsoids are at 50% probability). Hydrogens are omitted and carbons are not labeled for clarity.

Table 2. Selected bond lengths (Å) for **1**·$C_6H_5CH_3$ and **1**·$C_6H_5CH_3$·CH_3CN.

Atoms	**1**·$C_6H_5CH_3$	**1**·$C_6H_5CH_3$·CH_3CN	Atoms	**1**·$C_6H_5CH_3$	**1**·$C_6H_5CH_3$·CH_3CN
Co(1)–O(1)	1.926(2)	1.927(4)	Co(3)–O(11)	1.907(2)	1.902(4)
Co(1)–O(3)	1.872(2)	1.870(3)	Co(3)–N(5)	1.936(3)	1.931(4)
Co(1)–O(5)	1.914(2)	1.919(4)	Co(3)–N(6)	1.937(3)	1.941(4)
Co(1)–O(9)	1.901(2)	1.895(4)	Co(4)–O(2)	1.929(2)	1.908(3)
Co(1)–N(1)	1.937(3)	1.920(4)	Co(4)–O(4)	1.876(2)	1.866(4)
Co(1)–N(2)	1.929(3)	1.941(4)	Co(4)–O(8)	1.927(2)	1.921(4)
Co(2)–O(1)	1.926(2)	1.917(3)	Co(4)–O(12)	1.906(2)	1.911(4)
Co(2)–O(3)	1.870(2)	1.876(4)	Co(4)–N(7)	1.936(3)	1.933(5)
Co(2)–O(6)	1.911(2)	1.927(4)	Co(4)–N(8)	1.929(3)	1.925(4)
Co(2)–O(10)	1.910(2)	1.904(4)	Co(5)–O(3)	1.882(2)	1.881(3)
Co(2)–N(3)	1.949(3)	1.937(5)	Co(5)–O(4)	1.876(2)	1.884(4)
Co(2)–N(4)	1.925(3)	1.933(4)	Co(5)–O(9)	1.942(2)	1.940(3)
Co(3)–O(2)	1.927(2)	1.921(4)	Co(5)–O(10)	1.955(2)	1.935(4)
Co(3)–O(4)	1.873(2)	1.874(3)	Co(5)–O(11)	1.948(2)	1.942(3)
Co(3)–O(7)	1.916(3)	1.901(4)	Co(5)–O(12)	1.950(2)	1.944(4)

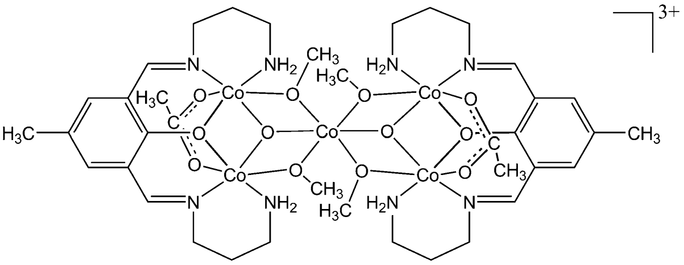

Figure 3. Structure of $[\{L(O_2CCH_3)Co_2O(OCH_3)_2\}_2Co]^{3+}$ (L^- = 2,6-bis((3-aminopropylimino)methyl)-4-methylphenolate).

group. The bridging oxo and the methoxo groups are so disposed that the $\{L(O_2CCH_3)Co_2O(OCH_3)_2\}$ unit becomes a tridentate O_3-donor facial ligand. The central Co(5) is in a distorted octahedral O_6 environment created by two such O_3-donor $\{L(O_2CCH_3)Co_2O(OCH_3)_2\}$ units (figure 3). The metal centers of each of the terminal dinuclear units are in two edge-shared N_2O_4 octahedra, while the central O_6 octahedron containing the fifth metal center shares two pairs of opposite edges with the four-terminal N_2O_4 octahedra. The pyramidal nature of each $\{Co_3(\mu_3\text{-}O)\}$ unit is indicated by the sum (~295°) of the three Co−O−Co bond angles. The metal centers Co(1)–Co(5) are not coplanar. The two triangles formed by these five metal centers are twisted at the shared Co(5) vertex. The dihedral angle between the two triangles is 72°. The Co···Co distances (≈2.781 Å) in the two dinuclear units are ~0.09 Å shorter than the distances (≈2.868 Å) between the central Co(5) and Co(1)−Co(4). The average of μ_3-oxo to Co(5) bond lengths (1.88 Å) is relatively much longer than that of μ_3-oxo to Co(1)−Co(4) bond lengths (1.87 Å). In contrast, the mean value of the μ_2-methoxo (O(9)−O(12)) to Co(5) bond lengths (1.94 Å) is relatively much longer than the mean value of the bond lengths involving O(9)−O(12) and Co(1)−Co(4) (1.90 Å). These differences indicate the somewhat loosely held nature of the trapped central metal. Stable discrete complexes containing cobalt(III) in an O_6 coordination environment as in **1** are very rare. To the best of our knowledge, the only other example of this type of complex is the trinuclear species $[\{\eta^5\text{-}CpCo(R_2PO)_3\}_2Co]^+$ where the central cobalt(III), which exhibits quintet–singlet spin crossover, is coordinated with two facial diamagnetic O_3-donor $\{\eta^5\text{-}CpCo(R_2PO)_3\}^-$ units ($Cp^- = C_5H_5^-$) [40].

3.3. *Spectroscopic characteristics*

The infrared spectrum of **1** recorded in a KBr pellet (figure S1, Supplementary data) shows two closely spaced bands at 3600 and 3540 cm^{-1} and a group of bands from 3260 to 2820 cm^{-1} due to the NH_2 and the C−H vibrations, respectively. The C=N stretch is located at 1640 cm^{-1} [41, 42]. The strong band at 1580 cm^{-1} is attributed to the bridging acetate asymmetric stretch. The band at 1470 cm^{-1} that overlaps with the broad and strong band centered at 1460 cm^{-1} is tentatively assigned to the symmetric stretch of the bridging acetate. The ClO_4^- anions in **1** show a characteristic strong broad band centered at 1080 cm^{-1} and the sharp strong band at 623 cm^{-1}.

The electronic spectrum of **1** in CH_3CN displays multiple bands from 400 to 200 nm (figure S2, Supplementary data). All the absorptions are intense, with the extinction coefficients (ε) in the order of 10^4–10^5 M^{-1} cm^{-1}. These bands are therefore likely to arise primarily from ligand-to-metal charge transfer and ligand-centered transitions [34, 43].

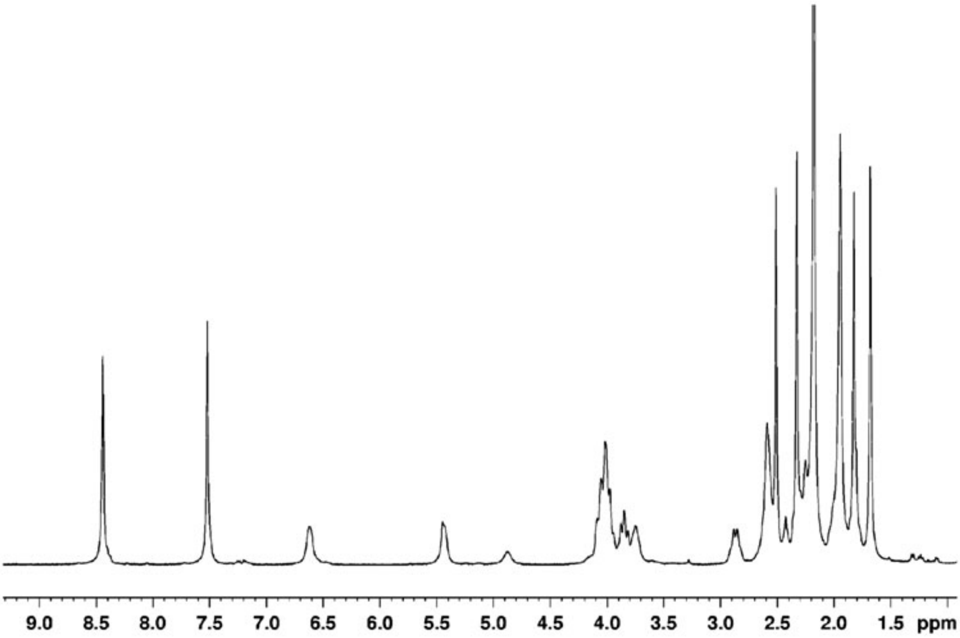

Figure 4. ^{1}H NMR spectrum of [{L(O_2CCH_3)$Co_2O(OCH_3)_2$}$_2$Co](ClO_4)$_3$ (**1**) in CD_3CN.

The ^{1}H NMR (400 MHz) spectrum of **1** was recorded in CD_3CN (figure 4). The azomethine protons and the phenolate *meta*-protons of the two L^- appear as two four-proton singlets at 8.44 and 7.52 ppm, respectively. The protons of the methyl groups at the *para* positions of the phenolate rings and the methyl protons of the two acetate bridges resonate as two singlets at 1.68 and 1.82 ppm, respectively. In contrast, the protons of the four bridging methoxo groups do not appear as a single signal, but instead as two singlets at 2.51 and 2.33 ppm. The multiplet (8H) centered at 4.01 ppm is attributed to the protons of the four methylene groups adjacent to the four azomethine groups. The broad singlet (8H) at 2.59 ppm is tentatively assigned to the protons of the central methylene groups of the four propylene fragments of the two dinucleating L^-. The protons of the methylene groups adjacent to the amine functionalities are observed at 3.85, 2.86, 2.42, and 2.25 ppm as a two-proton multiplet or a broad singlet. Four somewhat broad signals are observed at 6.61, 5.45, 4.87, and 3.75 ppm. The absence of these signals in the presence of D_2O indicates that these are the four NH_2 protons. The non-equivalent disposition is only observed for $–CH_2NH_2$ and the bridging methoxo group protons, which are nearest to the Co_5 core at the center of the cationic complex.

3.4. *Redox features*

The electron transfer characteristics of **1** have been studied by cyclic voltammetry. The measurements were carried out with a platinum disk working electrode, a platinum wire auxiliary electrode, and an Ag/AgCl reference electrode at 298 K under nitrogen for a ~10^{-3} M solution of **1** in CH_3CN with tetrabutylammonium perchlorate as the supporting electrolyte. The ferrocenium/ferrocene (Fc^+/Fc) couple was observed at $E_{1/2}$ = 0.50 V under

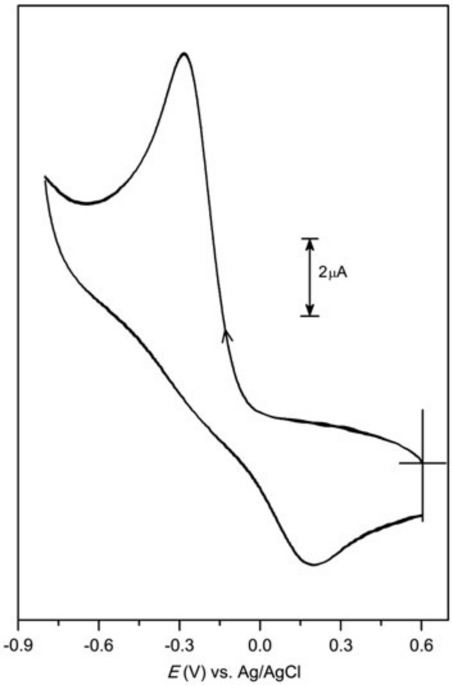

Figure 5. Cyclic voltammogram of $[\{L(O_2CCH_3)Co_2O(OCH_3)_2\}_2Co](ClO_4)_3$ at a scan rate of 100 mVs^{-1} using the experimental conditions described in the text.

identical conditions. The cyclic voltammogram of **1** displays a reduction response on the cathode side of the reference electrode (figure 5). The instability of the reduced species is indicated by the large cathodic peak current (i_{pc}) at $E_{pc} = -0.28$ V compared with the anodic peak current (i_{pa}) at $E_{pa} = 0.20$ V and the large ΔE_p ($= E_{pa} - E_{pc}$) value. Generally, ligand-based reductions of free as well as metal-coordinated Schiff bases are observed at much more negative potentials than the reduction response observed for **1** [43–47]. Indeed, a second irreversible broad reduction peak with E_{pc} centered at −1.25 V was observed on scanning the solution of **1** further, up to −2.0 V (figure S3, Supplementary data); thus this second reduction is most likely a ligand-centered process. The bond lengths in the X-ray structure of **1** indicate that the central cobalt(III) with a O_6 environment is somewhat weakly bonded, and hence less stable and more prone to reduction than the four-terminal cobalt(III) centers with N_2O_4 coordination geometry (*vide supra*). In addition, the i_{pc} of the first reduction is also comparable with the peak currents of Fc^+/Fc and other known one-electron redox processes [34, 48, 49]. Based on the above, the first response of **1** with $E_{1/2} = -0.04$ V is assigned to the reduction of the central $Co^{III}O_6$ to $Co^{II}O_6$.

4. Conclusion

A diamagnetic redox-active pentanuclear cobalt(III) coordination cluster $[\{L(O_2CCH_3)Co_2O(OCH_3)_2\}_2Co]^{3+}$ has been synthesized by a one-pot reaction. The cobalt(III) cluster comprises two dinucleating N_2ON_2-donor ligands L^-, two μ-acetato, two μ_3-oxo, and four

μ-methoxo ligands. The X-ray crystal structure shows that the two neutral dinuclear $\{L(O_2CCH_3)Co_2O(OCH_3)_2\}$ units create a distorted octahedral O_6 environment through their facially disposed oxo and methoxo groups, which coordinate the fifth cobalt(III) center. The bond parameters in addition to the redox behavior indicate that the central metal center is relatively weakly bonded and its +3 oxidation state is less stabilized compared with the metal centers in the dinuclear units. Our current efforts are focused on the synthesis of analogous hetero- and homometallic coordination clusters of other transition metal cations using HL and related Schiff bases.

Supplementary material

X-ray crystallographic data for $\mathbf{1}\cdot C_6H_5CH_3$ and $\mathbf{1}\cdot C_6H_5CH_3\cdot CH_3CN$ can be accessed from the CCDC (1003345 and 1003346, respectively). These data can be obtained free of charge via www.ccdc.cam.ac.uk/data_request/cif or from the Cambridge Crystallographic Data Center, 12 Union Road, Cambridge, CB2 1EZ, UK; Fax: (+44) 1223 336 033 or E-mail: deposit@ccdc.cam.ac.uk.

Acknowledgements

S. Maloth and S.K. Kurapati thank the Council of Scientific and Industrial Research for research fellowships.

Funding

This work was supported by the Department of Science and Technology (IYC grant and FIST program); and the University Grants Commission (CAS program).

Supplemental data

Supplementary figures S1–S3 can be found in the online version of this article. Supplemental data for this article can be accessed here [http://dx.doi.org/10.1080/00958972.2015.1018195].

References

[1] R.D. Adams, F.A. Cotton (Eds.). *Catalysis by Di- and Polynuclear Metal Cluster Complexes*, Wiley-VCH, New York (1998).

[2] A.D. Garnovskii, B.I. Kharisov, L.M. Blanco, A.P. Sadimenko, A.I. Uraev, I.S. Vasilchenko, D.A. Garnovskii. *J. Coord. Chem.*, **55**, 1119 (2002).

[3] G. Ambrosi, M. Formica, V. Fusi, L. Giorgi, M. Micheloni. *Coord. Chem. Rev.*, **252**, 1121 (2008).

[4] M.W. Cooke, G.S. Hanan. *Chem. Soc. Rev.*, **36**, 1466 (2007).

[5] V. Balzani, A. Juris, M. Venturi, S. Campagna, S. Serroni. *Chem. Rev.*, **96**, 759 (1996).

[6] A.F. Williams. *Chem. Met. Alloys*, **2**, 1 (2009).

[7] Y.-Z. Zheng, G.-J. Zhou, Z. Zheng, R.E.P. Winpenny. *Chem. Soc. Rev.*, **43**, 1462 (2014).

[8] R.A. Layfield. *Organometallics*, **33**, 1084 (2014) and references therein.

[9] S. Tanaka, H. Tsurugi, K. Mashima. *Coord. Chem. Rev.*, **265**, 38 (2014).

[10] M. Murrie. *Chem. Soc. Rev.*, **39**, 1986 (2010).

[11] G.E. Kostakis, S.P. Perlepes, V.A. Blatov, D.M. Proserpio, A.K. Powell. *Coord. Chem. Rev.*, **256**, 1246 (2012).

[12] M.-J. Niu, D.-W. Sun, H.-H. Li, Z.-Q. Cao, S.-N. Wang, J.-M. Dou. *J. Coord. Chem.*, **67**, 81 (2014).

[13] J.-C. Jiang, Z.-L. Chu, W. Huang, G. Wang, X.-Z. You. *Inorg. Chem.*, **49**, 5897 (2010).

[14] S. Majumder, S. Sarkar, S. Sasmal, E.C. Sañudo, S. Mohanta. *Inorg. Chem.*, **50**, 7540 (2011).

[15] A.K. Ghosh, R. Clérac, C. Mathonière, D. Ray. *Polyhedron*, **54**, 196 (2013).

[16] A.K. Ghosh, M. Pait, R. Clérac, C. Mathonière, V. Bertolasi, A. Bauzá, A. Frontera, K. Pramanik, D. Ray. *Dalton Trans.*, **43**, 4076 (2014).

[17] S.S. Tandon, S.D. Bunge, R. Rakosi, Z. Xu, L.K. Thompson. *Dalton Trans.*, 6536 (2009).

[18] L.-L. Hu, Z.-Q. Jia, J. Tao, R.-B. Huang, L.-S. Zheng. *Dalton Trans.*, 6113 (2008).

[19] M. Dincă, T.D. Harris, A.T. Iavarone, J.R. Long. *J. Mol. Struct.*, **890**, 139 (2008).

[20] I.C. Lazzarini, A.V. Funes, L. Carrella, L. Sorace, E. Rentschler, P. Alborés. *Eur. J. Inorg. Chem.*, 2561 (2014).

[21] X. Xy, Y. Ma, Y. Lu, E. Wang. *J. Coord. Chem.*, **60**, 1005 (2007).

[22] L. Tian, L. Yan. *J. Coord. Chem.*, **65**, 1600 (2012).

[23] S.-D. Han, W.-C. Song, J.-P. Zhao, Q. Yang, S.-J. Liu, Y. Lia, X.-H. Bu. *Chem. Commun.*, **49**, 871 (2013).

[24] M. Lamouchi, E. Jeanneau, G. Novitchi, D. Luneau, A. Brioude, C. Desroches. *Inorg. Chem.*, **53**, 63 (2014).

[25] D. Sahoo, R.K. Metre, W. Kroener, K. Gieb, P. Müller, V. Chandrasekhar. *Eur. J. Inorg. Chem.*, 2490 (2014).

[26] Bruker-Nonius Analytical X-ray Systems Inc. *SMART (V5.630) and SAINT-Plus (V6.45)*, Madison, WI (2003).

[27] G.M. Sheldrick. *SADABS, Program for Area Detector Absorption Correction*, University of Göttingen, Göttingen (1997).

[28] Oxford Diffraction Ltd. *CrysAlisPro (V1.171.35.19)*, Abingdon (2011).

[29] G.M. Sheldrick. *Acta Crystallogr., Sect. A*, **64**, 112 (2008).

[30] L.J. Farrugia. *J. Appl. Crystallogr.*, **32**, 837 (1999).

[31] A.L. Spek. *PLATON A Multipurpose Crystallographic Tool*, Utrecht University, Utrecht, The Netherlands (2002).

[32] C.F. Macrae, I.J. Bruno, J.A. Chisholm, P.R. Edgington, P. McCabe, E. Pidcock, L. Rodriguez-Monge, R. Taylor, J. van de Streek, P.A. Wood. *J. Appl. Crystallogr.*, **41**, 466 (2008).

[33] W.J. Geary. *Coord. Chem. Rev.*, **7**, 81 (1971).

[34] S.G. Sreerama, D. Shyamraj, S.N. Pal, S. Pal. *Indian J. Chem.*, **42A**, 2352 (2003).

[35] J.K. Beattie, J.A. Klepetko, A.F. Masters, P. Turner. *Polyhedron*, **22**, 947 (2003).

[36] A.M. Goforth, R.E. Hipp, M.D. Smith, L. Peterson Jr., H.-C. zur Loye. *Acta Crystallogr., Sect. E*, **61**, m1531 (2005).

[37] J. Luo, N.P. Rath, L.M. Mirica. *Inorg. Chem.*, **50**, 6152 (2011).

[38] S. Paul, W.-T. Wong, D. Ray. *Inorg. Chim. Acta*, **372**, 160 (2011).

[39] M. Salehi, R. Kia, A. Khaleghian. *J. Coord. Chem.*, **65**, 3007 (2012).

[40] W. Klaeui, W. Eberspach, P. Guetlich. *Inorg. Chem.*, **26**, 3977 (1987) and references therein.

[41] F. Hueso-Ureña, N.A. Illán-Cabeza, M.N. Moreno-Carretero, J.M. Martínez-Martos, M.J. Ramírez-Expósito. *J. Inorg. Biochem.*, **94**, 326 (2003).

[42] Z.-L. Wang, Q.-H. Luo, C.-Y. Duan, C.-Y. Shen, Y.-Z. Li. *Dalton Trans.*, 1104 (2004).

[43] J. Chakraborty, R.K.B. Singh, B. Samanta, C.R. Choudhury, S.K. Dey, P. Talukder, M.J. Borah, S. Mitra. *Z. Naturforsch.*, **61b**, 1209 (2006).

[44] J.M.W. Scott, W.H. Jura. *Can. J. Chem.*, **45**, 2375 (1967).

[45] J. Lewis. M, Schröder, *J. Chem. Soc., Dalton Trans.*, 1085 (1982).

[46] K. Ding, Q. Wang, Z. Jia, R. Tong, X. Wang, H. Shao. *J. Chin. Chem. Soc.*, **50**, 387 (2003).

[47] A. Vijayaraj, R. Prabu, R. Suresh, R.S. Kumari, V. Kaviyarasan, V. Narayanan. *Bull. Korean Chem. Soc.*, **33**, 3581 (2012).

[48] B.K. Panda. *J. Chem. Sci.*, **116**, 245 (2004).

[49] A.R.B. Rao, S. Pal. *J. Organomet. Chem.*, **762**, 58 (2014).